Integration of Amorphous Silicon Photosensors with Thin Film Interferential Filter for Biomolecule Detection

Domenico Caputo[1(✉)], Emanuele Parisi[1], Augusto Nascetti[2], Mario Tucci[3], and Giampiero de Cesare[1]

[1] D.I.E.T., University of Rome "La Sapienza", via Eudossiana 18, 00184 Rome, Italy
domenico.caputo@uniromal.it
[2] S.A.E., University of Rome "La Sapienza", via Salaria 851/881, 00138 Rome, Italy
[3] ENEA Research Center Casaccia, via Anguillarese 301, 00123 Rome, Italy

Abstract. This work presents a thin film device, combining, on the same glass substrate, photosensors and long-pass interferential filter to achieve a compact and efficient sensor for biomolecule detection. The photosensors are amorphous silicon stacked structures, while the interferential filter is fabricated alternating layers of silicon dioxide and titanium dioxide, directly grown over the photosensors. The system has been optimized to effectively detect the natural fluorescence of Ochratoxin A, a highly toxic mycotoxin present in different food commodities. In particular, the long-pass interferential filter has been designed to reject the wavelengths arising from the excitation source (centered at 330 nm) thus transmitting the OTA emission spectrum (centered at 470 nm). Experimental results show that the filter strongly reduces the photosensors quantum efficiency below 420 nm, while keeps it nearly constant at higher wavelength.

Keywords: Thin film · Amorphous silicon · Interferential filter · Photosensors · Ochratoxin A

1 Introduction

Detection techniques of biomolecules have received and continue to receive a great attention due to their relevance in biology, chemistry, medicine and agriculture. Therefore, innovative methods are coming up beside the standard techniques [1]. As an example, in food related applications, established procedures rely on enzyme-linked immunosorbent assay (ELISA) or on chromatographic procedures. The ELISA kit [2, 3] are usually competitive enzyme immunoassays based on specific antibodies optimized to cross react primarily with the target molecules, while the chromatographic techniques rely on high-performance liquid chromatography (HPLC), through extraction of the analyte from the sample, clean-up (or purification) by ImmunoAffinity Columns (IAC) [4] and chromatographic analysis. ELISA based method are

B. Andò et al. (eds.), *Sensors*, Lecture Notes in Electrical Engineering 431,
DOI 10.1007/978-3-319-55077-0_16

friendly-to-use, less expensive and less time-consuming than HPLC techniques, which on the other hand are much more reliable in terms of analyte quantification.

To overcome the disadvantages of these standard methods, many research efforts are currently committed to develop lab-on-chip (LoC) systems [5, 6], integrating on single substrate devices and techniques for the thermal treatment [7], handling, recognition and quantification of biomolecules [8]. The main advantages of the LoC are the low reagent consumption and the shortening of analysis time. These characteristics coupled with the possibility to automatize the analysis procedure make LoCs the ideal systems easy-to-use, low-cost and low pollution devices. However, even though LoCs tend to be as compact as possible, their scaling down is slowed by the need of bulky external connections [9] and off-chip detection [10].

Our work addresses the effective LoC miniaturization integrating, on the same glass substrate, amorphous silicon (a-Si:H) photosensors [11–15] and interferential filter to achieve on-chip detection of fluorescent molecules. In particular, the integrated device has been developed for the detection of Ochratoxin A (OTA) [16], a mycotoxin present in different food commodities such as red wine, beer, coffee and peanuts. Indeed OTA has received a great attention by scientists and dietary organizations, because this mycotoxin is carcinogenic (Group 2B) [17], can have weak mutagenic effects [18] and immunotoxicity activity in animals [19].

2 Device Structure

The device structure is showed in Fig. 1. The system is designed to detect the natural fluorescence of OTA molecules by means of a-Si:H photosensors.

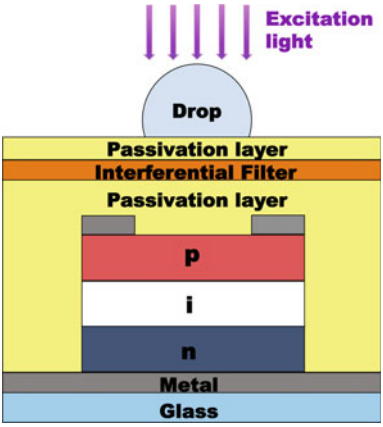

Fig. 1. Device structure

An appropriate radiation source excites the fluorescence of OTA molecules contained in a solution drop, while the thin film interferential filter, integrated onto the structure, rejects the excitation radiation and only transmits the OTA fluorescence. The a-Si:H photosensors absorb the transmitted light and generate photocarriers collected at

the metal electrodes, giving rise to a current proportional to the number of photons and then to the number of OTA molecules contained into the drop.

The design of photosensors and filter started from the OTA emission and absorption spectra shown in Fig. 2. The absorption spectrum is centered at 330 nm, while the emission spectrum is centered at 470 nm.

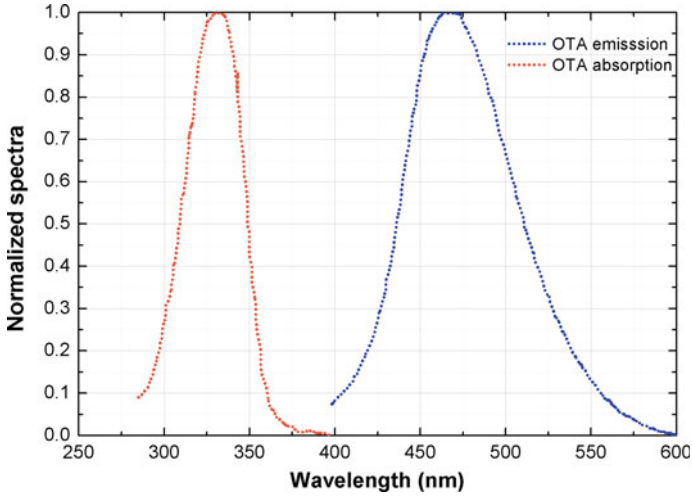

Fig. 2. Emission (*orange dotted line*) and absorption (*blue dotted line*) spectra of Ochratoxin A (Color figure online)

From these data, we infer the requirements for the excitation source, the spectral response of the photodiodes and the interferential filter. A laser diode or a light emitting diode, able to provide an ultraviolet light, is chosen as excitation source.

3 Amorphous Silicon Photodiodes

The photosensors used to detect the emission of OTA are a-Si:H photodiodes. Their structure is a p-type/intrinsic/n-type (p-i-n) stacked junction, deposited by Plasma Enhanced Chemical Vapor Deposition (PECVD) at temperatures below 300 °C. The deposition parameters are listed in Table 1.

The thicknesses and energy gaps of the different layers within the a-Si-H device have been tuned to maximize the matching between OTA emission spectrum and photosensor quantum efficiency, keeping the dark current as low as possible.

The achieved quantum yield (QY) is showed in Fig. 3 as black squares. The measured value at 470 nm is 185 mA/W. The current density, measured in dark conditions at 100 mV of low reverse voltage, is in the order of 10^{-10} A/cm^2. This reflects in a dark current noise in the order of few fA/cm^2.

Table 1 Deposition parameters of the a-Si:H layers

Material	SiH_4 (sccm)	B_2H_6 (sccm)	CH_4 (sccm)	PH_3 (sccm)	T_{dep} (° C)	P_{dep} (Torr)	P_{RF} (mW/cm^2)	t_{dep} (s)
p/a-SiC:H	40	5	40		210	0.7	25	50
i/a-Si:H	40				280	0.68	25	2100
n/a-Si:H	40			10	300	0.3	25	180

The gases are: SiH_4 pure silane, PH_3 silane diluted (5%), B_2H_6 helium diluted (5%), CH_4 pure methane. P_{dep} is the process pressure, P_{RF} the radio-frequency power density, T_{dep} the substrate temperature and t_{dep} the deposition time

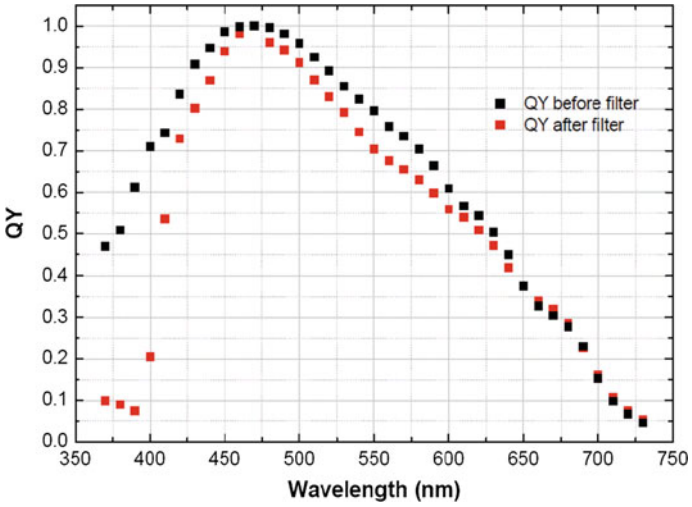

Fig. 3. Quantum yield of the a-Si:H photodiodes before (*black squares*) and after (*red squares*) the deposition of the interference filter (Color figure online)

4 Interferential Filter Design

As can be deduced comparing Figs. 2 and 3, the quantum yield of the photosensors is not negligible in the absorption spectrum of the OTA molecules, therefore a long-pass filter is necessary to reject the light coming from the excitation source.

The modeled thin-film filter is a multi-dielectric interferential filter, designed according to Distributed Bragg Reflector's theory (DBR). The periodic structure is composed by alternating two films with high and low refractive index. The optical thickness of the two layers is equal to a quarter of the incident wavelength.

$$n_h d_h = n_l d_l = \lambda_0/4$$

where n_h and d_h are, the refractive index and the thickness of high refractive index layer respectively, n_l and d_l are, the refractive index and the thickness of low refractive index layer respectively, $\lambda_0 = c_0/f_0$ is the wavelength of the incident radiation.

The wavelength-pass region can be made flat by setting the thicknesses of the first and last high-index layers equal to $\lambda_0/8$. The filter response has been modeled with the IMD extension of the freeware software XOP. The chosen materials are TiO_2 and SiO_2 and the designed filter structure is schematically reported in Fig. 4.

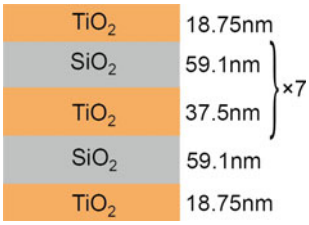

Fig. 4. Structure of the thin film multi-dielectric interferential OTA filter

The modeled transmittance (T) and reflectance (R), reported as continuous lines in Fig. 5, show that the filter provides a stop-band attenuation of three orders of magnitude (optical density OD = 3.0 at 340 nm). Furthermore, its cut-off wavelength (50% of T) is 408 nm, while the roll-off (20 nm from 10 to 90% of T) permits an almost unperturbed transmission of the OTA emission.

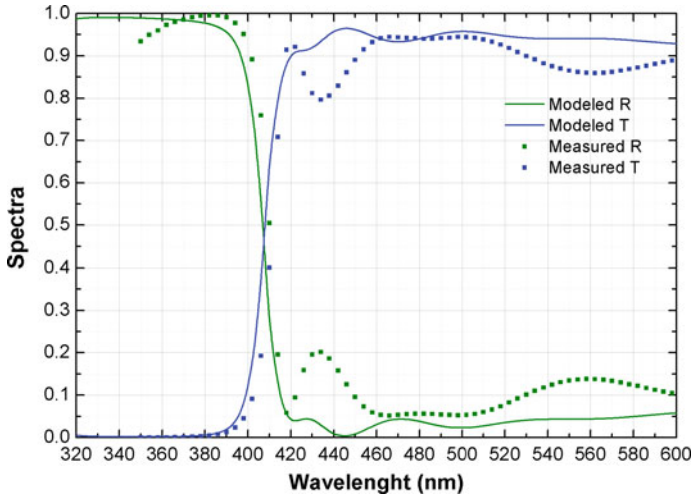

Fig. 5. Modeled (*continuous lines*) and measured (*symbols*) spectral characteristics of the interferential filter

5 Experimental Results

At first, the designed filter has been deposited by Electron Beam Physical Vapor Deposition at 250 °C on a plain borosilicate glass. This deposition temperature is lower than the maximum temperature reached during the a-Si:H photosensors fabrication. The spectral characteristics of the filter have been then measured with a *Perkin Elmer Lambda 950* spectrophotometer.

The measured transmittance (T) and reflectance (R) are showed in Fig. 5 as blue and green squares, respectively. An excellent agreement between measurements and simulations has been achieved. Indeed, both the measured cut-off wavelength and the stop-band attenuation are very close to the simulated value, thus demonstrating that the fabricated filter satisfies very well the design requirements.

Finally, using the same deposition parameters adopted for the plain borosilicate glass, the filter has been deposited directly onto the photosensors. The spectral response, measured after the filter deposition, is reported as red squares in Fig. 3. We can observe that the quantum efficiency remains almost unchanged in the OTA emission range, while it experiments a sharp decrease at wavelength below 420 nm. These data confirm, therefore, the filter effectiveness in rejecting the excitation radiation and its successful integration with the photosensors.

6 Conclusion

This work has reported design, fabrication and characterization of a device based on thin film technologies suitable for selective detection of the natural fluorescence of Ochratoxin A molecules. A multi dielectric interferential long-pass filters have been designed through a freeware software, according to Distributed Bragg Reflector's theory. The filter, directly deposited onto an a-Si:H photosensors array, is able to reject the excitation UV light and to transmit the OTA emission light. Indeed the filter measurements show excellent agreement with simulations.

The photodiode quantum yield, measured before and after the filter deposition, demonstrates the successful integration of filter with sensors and the suitability of the system to effectively reject the excitation radiation thus accomplishing the specimen desired. Works are currently in progress to test the performances of the integrated device on standard samples of Ochratoxin A.

References

1. F. Costantini, C. Sberna, G. Petrucci, C. Manetti, G. de Cesare, A. Nascetti, D. Caputo, Lab-on-chip system combining a microfluidic-ELISA with an array of amorphous silicon photosensors for the detection of celiac disease epitopes. Sens. Bio-Sens. Res. **6**, 51–58 (2015)
2. http://www.sigmaaldrich.com/catalog/product/sigma/se120014?lang=it&region=IT
3. http://www.biooscientific.com/Mycotoxin-test-kits/MaxSignal-Ochratoxin-A-ELISA-Test-Kit

4. H. Meng, Z. Wang, S. De Saeger, Y. Wang, K. Wen, S. Zhang, J. Shen, Determination of Ochratoxin A in cereals and feeds by ultra-performance liquid chromatography coupled to tandem mass spectrometry with immunoaffinity column clean-up. Food Anal. Methods **7**(4), 854–864 (2014)
5. A. Manz, N. Graber, H.M. Widmer, Miniaturized total chemical-analysis systems—a novel concept for chemical sensing. Sens. Actuat. B-Chem. **1**(1–6), 244–248 (1990)
6. L. Gervais, N. de Rooij, E. Delamarche, Microfluidic chips for point-of-care immunodiagnostics. Adv. Mater. **23**(24), H151–H176 (2011)
7. D. Caputo, G. de Cesare, M. Nardini, A. Nascetti, R. Scipinotti, Monitoring of tempera-ture distribution in a thin film heater by an array of a-Si: H temperature sensors. IEEE Sens. J. **12** (5), 1209–1213 (2012)
8. D. Caputo, M. Ceccarelli, G. de Cesare, A. Nascetti, R. Scipinotti, Lab-on-Glass system for DNA analysis using thin and thick film technologies. Proceedings of material research symposium, vol. 1191, OO06-01 (2009)
9. K. Lewotsky, Microfluidics streamlines laboratory operations. SPIE Newsroom (2010). doi:10.1117/2.2201012.01
10. F. Berthold, M. Hennecke, J. Wulf, Instrumentation for chemi-luminescence and bioluminescence, in *Chemiluminescence and Bioluminescence—Past, Present and Future*, ed. by A. Roda (RSC, Cambridge, 2011), pp. 113–139
11. D. Caputo, G. de Cesare, A. Nascetti, R. Negri, Spectral tuned amorphous silicon p-i-n for DNA detection. J. Non-Cryst. Solids **352**(9-20 SPEC. ISS.), 2004–2006 (2006)
12. A.C. Pimentel, A.T. Pereira, V. Chu, D.M.F. Prazeres, J.P. Conde, Detection of chemiluminescence using an amorphous silicon photodiode. IEEE Sens. J. **7**(3–4), 415–416 (2007)
13. C.R. Vistas, S.S. Soares, R.M.M. Rodrigues, V. Chu, J.P. Conde, G.N.M. Ferreira, An amorphous silicon photodiode microfluidic chip to detect nanomolar quantities of HIV-1 virion infectivity factor. Analyst **139**(15), 3709–3713 (2014)
14. F. Costantini, A. Nascetti, R. Scipinotti, F. Domenici, S. Sennato, L. Gazza, F. Bordi, N. Pogna, C. Manetti, D. Caputo, G. de Cesare, On-chip detection of multiple serum antibodies against epitopes of celiac disease by an array of amorphous silicon sensors. RSC Adv. **4**(4), 2073–2080 (2014)
15. M. Mirasoli, A. Nascetti, D. Caputo, M. Zangheri, R. Scipinotti, L. Cevenini, G. de Cesare, A. Roda, Multiwell cartridge with integrated array of amorphous silicon photosensors for chemiluminescence detection: development, characterization and comparison with cooled-CCD luminograph. Anal. Bioanal. Chem. **406**(23), 5645–5656 (2014)
16. D. Caputo, G. de Cesare, C. Fanelli, A. Nascetti, A. Ricelli, R. Scipinotti, Innovative detection system of ochratoxin a by thin film photodiodes. Sensors **7**(7), 1317–1322 (2007)
17. H.A. Clark, S.M. Snedeker, Ochratoxin A: its cancer risk and potential for exposure. J. Toxicol. Environ. Health. Part B, Crit. Rev. **9**(3), 265–296 (2006)
18. N. Palma, S. Cinelli, O. Sapora, S.H. Wilson, E. Dogliotti, Ochratoxin A-induced mutagenesis in mammalian cells is consistent with the production of oxidative stress. Chem. Res. Toxicol. **20**(7), 1031–1037 (2007)
19. L. Al-Anati, E. Petzinger, Immunotoxic activity of ochratoxin A. J. Vet. Pharmacol. Ther. **29** (2), 79–90 (2006)